Journal of Materials Chemistry C

Accepted Manuscript

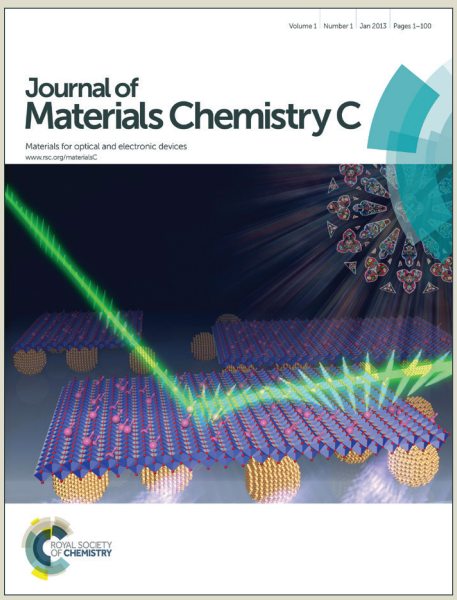

ROYAL SOCIETY OF CHEMISTRY

www.rsc.org/materialsC

Extremely High Color Rendering White Light from Surface Passivated Carbon Dots and Zn-doped $AgInS_2$ Nanocrystals

Wonkeun Chung, Hyunchul Jung, Chang Hun Lee, and Sung Hyun Kim*

Department of Chemical and Biological Engineering, Korea University,

1 Anam-Dong, Seongbuk-Gu, Seoul 136-713, Korea

*Corresponding author. Tel.: +82-02-3290-3297; fax: +82-02-926-6102

E-mail address: kimsh@korea.ac.kr (S.H. Kim)

Abstract

In this study, highly luminescent carbon dots with diameters of 3–5 nm were synthesized via the carbonization of citric acid, and the effects of the surface passivation and carbonization temperature on the optical properties were investigated. A red-shift in the emission wavelength was observed with increasing excitation wavelength, and oleylamine-capped carbon dots showed the highest quantum yield of approximately 43% when excited at 380 nm, whereas the reaction temperature had no influence on the emission wavelength and morphology of the dots. Additionally, I-III-VI $AgInS_2$ nanocrystals (NCs) were prepared by thermal decomposition at a low temperature, and the emission wavelength was tuned by adjusting the growth temperature or introducing Zn ions, which enhanced the quantum yield up to 50%. For carbon dot application, a white LED was fabricated by combining a 380nm UV LED with the carbon dots and Zn-doped $AgInS_2$ NCs. The white light from this LED exhibited an excellent color rendering index of greater than 95 with a warm color temperature, and demonstrated its potential for use in solid state lighting.

Keywords: carbon dots, surface passivation, white light emitting diodes

1. Introduction

Recently, non-toxic semiconductor nanocrystals (NCs) have been widely investigated as potential alternatives to CdSe-based NCs. In particular, I-III-VI semiconductor NCs such as $CuInS_2$ (1.5 eV), $CuInSe_2$ (1.05 eV), and $AgInS_2$ (1.8 eV) have been studied for optoelectronic and biological applications because of their suitable band-gap energy, high absorption coefficients, and radiation stability [1-11]. Among these, $AgInS_2$ NCs have a direct band gap range of 1.87–2.03 eV, depending on their crystal structure, and exhibit a distinctive absorption in the visible region or near-infrared region, along with an emission wavelength that can be tuned by changing the size or composition. Additionally, $AgInS_2$ NCs can be obtained at relatively low temperatures because of the high reactivity of silver ions with sulfur. Vittal et al. first reported the fabrication of orthorhombic $AgInS_2$ NCs through the thermal decomposition of a single-source precursor of $[(Ph_3P)_2AgIn(SCOPh)_4]$ [5], after which Torimoto et al. obtained color adjustable ZnS–$AgInS_2$ NCs through the thermal decomposition of $(AgIn)_xZn_{2(1-x)}(S_2CN(C_2H_5)_2)_4$ [6]. Recently, a high quantum yield of tunable ZnS-$AgInS_2$ NCs was synthesized by Zn diffusion into an $AgInS_2$ lattice [8-10].

Apart from the traditional binary or ternary semiconductor NCs, carbon nanodots with diameters below 10 nm are emerging as new luminescent nanomaterials because of their low toxicity, chemical inertness, high thermal and photo stabilities, abundant and inexpensive sources, and biocompatibility [12-17]. Scrivens et al. first obtained nano-size fluorescent carbon particles by the purification of single-walled carbon nanotubes from arc-discharge soot [18]. Since then, various synthetic methods have been developed, which can be classified into two approaches: i) top-down and ii) bottom-up approaches. Top-down approaches include arc-discharge [18], laser-ablation [12, 19], plasma treatment [20], and electrochemical methods [13], and bottom-up approaches include combustion/thermal [21-23], microwave [15], and supported methods [24]. Fundamental studies and synthetic methods for carbon dots have attracted tremendous interest. However, the use of carbon dots in light emitting diode (LED) applications is rarely reported. Ma et al. fabricated an electroluminescent white LED by employing carbon dots as the emission layer, and showed a color

rendering index (CRI) of 82 with a high turn-on voltage of 6 V [21]. More recently, Rogach et al. reported a color-switchable carbon-based electroluminescent LED [25]. Chen's and Rhee's groups demonstrated color-conversion white LEDs by combining LED chips with a carbon dot condensed film [26] or carbon dot-PMMA film [27]. However, the results could not meet the general lighting demand for a high CRI with warm white light.

In this study, nano-sized highly luminescent carbon dots were synthesized via facile thermal carbonization using the citric acid method, and the effects of the surface passivation and carbonization temperature on the optical properties were investigated. Then, we demonstrated a color-conversion white LED by using carbon dots as a potential color converter. Furthermore, Zn-doped $AgInS_2$ NCs were added to improve the color quality, and we explored their potential for LED application.

2. Experimental

Carbon dots were synthesized by the thermal carbonization of citric acid in a noncoordinating solvent with different capping agents [21]. A mixture of 1-hexadecylamine (HDA, 1.5g) or oleylamine (OAm, 1.84 ml) and octadecene (ODE, 10 mL) was heated to 150°C under an N_2 condition, and citric acid (1 g) was injected. The reaction temperature was raised to 300°C, and then kept at this reaction temperature for 180 min. The obtained carbon dots were washed out with acetone several times.

$AgInS_2$ NCs were synthesized by the thermal decomposition of silver nitrate (0.2 mmol), indium acetate (0.2 mmol), and 1-dodecanethiol (0.5 mmol) in a mixture of ODE (6 mL), trioctylphosphine (TOP, 0.1 mL), and oleic acid (0.1 mL), which acted as a solvent and surfactants [9]. Sulfur powder (4 mmol) dissolved in ODE (2mL) was injected at 100°C and heated to the desired temperature. To introduce the Zn ion, zinc stearate (0.8, 0.4, 0.2, and 0.1 mmol) dissolved in OAm (3 mL) was added at 130°C, and the reaction temperature was maintained for 20 min for the Zn diffusion. The obtained Zn-doped $AgInS_2$ NCs were isolated by adding chloroform/methanol (1:1 vol:vol) mixture, and then precipitated by acetone. The prepared carbon dots and Zn-doped $AgInS_2$ NCs were redispersed in chloroform (1 mg/mL), and measured their optical properties.

For fabrication of white LED, emitting nanoparticles were physically mixed with poly(methyl methacrylate) (PMMA, M_w=996,000) in chlorobenzene. The emitting nanoparticles and PMMA (1:10 wt%) mixtures were sonicated for homogenous dispersion in PMMA matrix, and dropped onto an LED chip.

3. Results and Discussion

To investigate the surface effect on the luminescence properties, HDA-, OAm-, and mercaptopropionic acid (MPA)-capped carbon dots were prepared. OAm and HDA have a primary amine group, and play roles as stabilizing ligands, as well as in controlling the shape of the nanostructure [28]. As shown in figure 1, HR-TEM image (Tecnai 20), HDA- and OAm-capped carbon dots are nearly spherical in shape, with diameters of 3–5 nm. However, the OAm-capped carbon dots showed a better uniform morphology and size distribution. Furthermore, the X-ray diffraction (ATX-G, Rigaku, with Cu Kα radiation) shown in figure S1, HDA-capped carbon dots showed the poor crystallization, and (002) interlayer spacing was 4.18 Å, which was larger than that of bulk graphite (3.3 Å) due to the introduction of oxygen containing functional group [16].

From the FT-IR (ThermoFisher Scientific Nicolet IS10) spectra in figure 2(a) and (b), both the HDA- and OAm-capped carbon dots showed a broad amide band, with peaks at 3100–3500 cm^{-1} for the N-H stretch, 1640 cm^{-1} for the N-H bend, 1680–1710 cm^{-1} for the C=O stretch, and 1250–1370 cm^{-1} for the C-N stretch, indicating that carbonyl groups were converted into amide groups by passivating with OAm or HDA. The two strong sharp peaks observed at 2921 and 2852 cm^{-1} were C-H vibrations of the aliphatic groups. MPA-capped carbon dots were prepared via ligand exchange. OAm-capped carbon dots dispersed in chloroform and excess MPA were sonicated in methanol at 80°C (with tetramethylammonium hydroxide pentahydrate (TMAH) used to adjust the pH), which resulted in the removal of OAm and rendered water soluble property. The peaks at 1568 and 1397 cm^{-1} were COO^- symmetric and asymmetric stretches, respectively, which produced the water solubility. The weak

peak of the mercaptans S-H stretch presented at 2550 cm^{-1} indicates that the MPA ligands were deprotonated and attached to the surface [29].

The absorption (PerkinElmer Lambda 35) and emission (PerkinElmer LS 55) spectra of the OAm-, HDA-, and MPA-capped carbon dots are given in figure 3. The HDA- and OAm-capped carbon dots (dispersed in chloroform) showed broad absorption bands with distinct absorption peaks at 369 nm, and 373 nm, respectively. The emission mechanism of carbon dots is not yet fully understood. However, the emission wavelength is strongly dependent on the excitation energy [12-27]. The typical emission behavior was observed in the OAm- and HDA-capped carbon dots, and predominantly, the emission wavelength of the OAm-capped carbon dots was longer than that of the HDA-capped carbon dots. The emission band was asymmetric and quite broad, with a full width at half maximum (FWHM) over 100 nm, and shifted to longer wavelengths with increasing excitation wavelength as a result of the size distribution from the quantum effect, different emissive traps on the surface, and/or pyrolytic formation of several different fluorophores within the carbon dots [20-22]. At a shorter excitation wavelength (<380nm), two peaks were observed near 440 and 480 nm, and a slight emission shift occurred. In contrast, at a longer excitation wavelength, the emission band became narrower, and a large emission shift was observed at excitation wavelength between 400 and 500nm. The previous works suggested that the energy levels of the surface trap states are closely related to the functional groups [14-17, 21]. HDA- and OAm-capped carbon dots have a chemical similarity, except for the hydrocarbon length and double bonding of OAm. While the surfaces of MPA-capped carbon dots are functionalized with –OH groups, and –SH groups bind to the surfaces. Accordingly, the optical properties of the MPA-capped carbon dots were distinguished from the OAm- and HDA-capped carbon dots. The absorption spectrum of the MPA-capped carbon dots (dispersed in D.I. water) was broad with a sharp peak at 360 nm. In addition, the emission position was weakly dependent on the excitation wavelength in the UV excitation region. Only 3 nm of red-shift was observed within the range $365 < \lambda_{ex} < 400$nm. The quantum yield of the MPA ligand exchanged carbon dots was 9%, whereas the yields were 43% and 37% in the OAm- and HDA-capped carbon dots, respectively, under an exciting source at 380 nm.

Lee et al. reported the relationship between the HOMO-LUMO gap and the dot size in a graphite fragment of carbon quantum dots [13]. To investigate the size-dependent optical properties in this case, carbon dots were synthesized at different reaction temperature (200, 250, and 300°C). In general, the emission of semiconductor NCs is dependent on their size, and the emission wavelength can be controlled by the growth temperature and/or time. However, no significant change in size was observed with increasing reaction temperature. The size of the OAm-capped carbon dots remained approximately 3–5 nm, regardless of the reaction temperature, which indicated that the formation of the carbon dots did not follow the ostwald ripening mechanism. The preparation of carbon dots using this method underdoes depolymerization, decomposition, and pyrolysis processes, with the formation of a gas and condensable vapor phase [21]. Thus, the reaction temperature could not play an important role in tuning the size of the carbon dots. As shown in figure 4, the carbonization temperature (200~300^{o}C) had no strong influence on the emission properties.

Figure 5 shows the PL spectra of $AgInS_2$ NCs obtained with different reaction temperatures and Zn ratios. The emission of $AgInS_2$ was observed without sulfur powder injection, because the DDT acted as a sulfur source as well as a stabilizing ligand by forming thiolates with various metal salts. However, this excess sulfur source led to a large amount of burst nucleation, and greatly improved the quantum yield from ~3% to 15%. The growth of the $AgInS_2$ NCs conformed to the ostwald ripening mechanism. Thus, the size of the NCs became larger with increasing reaction temperature, and a corresponding red-shift was observed due to the reduction in the quantum confinement effect.

The XRD pattern, in figure 6, of $AgInS_2$ and Zn-doped $AgInS_2$ obtained at 130°C was quite broad because of the nano-size particles and poor crystallinity. The $AgInS_2$ NCs showed strong broad peaks around 2θ values of 24.2°, 26.4°, and 28.3°, which were orthorhombic structures of the (120)/(200), (002), and (121)/(201) phases, respectively. Also, broad peaks were observed around 2θ=44.4-48.1° corresponding to (040), (320), and (123) phase of orthorhombic $AgInS_2$ NCs. After the Zn introduction at Zn/Ag=4, three main peaks were observed around 2θ values of 28.4°, 47.6° and 56.1°, which coincided with the (111), (200), and (311) phases of the cubic structure (zinc blend), suggesting that a phase transition from orthorhombic to cubic occurred. After the Zn introduction, the size and

shape were retained below a diameter of 7 nm, with a spherical shape, as shown in the HR-TEM image.

The alloying of components with a higher band gap (ZnS, 3.54 eV) and a lower band gap ($AgInS_2$, orthorhombic, 1.87 eV) could tune the band gap. As the Zn/Ag (=In) ratio was increased from 0.5 to 2, the absorption onset of the NCs was notably blue-shifted, and the emission wavelength was also blue-shifted from 644 (pure $AgInS_2$ NCs) to 634, 618, 582, and 539 nm. In addition, substituting Zn ions for Ag and/or In ions could inhibit the generation of vacancies, and reduce the defects in $AgInS_2$ NCs. Thus, the quantum yields of the Zn-doped $AgInS_2$ NCs, relative to Rhodamine 6G, were 35% (634 nm), 51% (618 nm), 45% (582 nm), and 29% (539 nm), which were much higher than that of $AgInS_2$ NCs (13%).

For practical application, carbon dots were used in a bluish-green emitter under 380nm UV LED excitation, as well as in a yellow emitter under 430nm blue LED excitation. When carbon dots were integrated with a 430nm LED, a CIE coordinate of (0.3385, 0.3062) and correlated color temperature (CCT) of 5044 K for cool white light were obtained at 50 mA (Lab sphere, CDS1100). Because of the broad emission band, CRI reached 77.4, comparable to a YAG-based white LED, and better than a single yellow-emitting $CuInS_2$-based NC [2] white LED. Additionally, a 380nm UV LED pumped white LED was fabricated by combining carbon dots and a 618nm emitting Zn-doped $AgInS_2$ NC emitter (carbon dots : $ZnAgInS_2$ NCs = 4:1 wt%). For preventing the energy transfer among the emissive nanoparticles, lower energy of red emissive Zn-doped $AgInS_2$ NCs was first coated onto LED chip, followed by higher energy of bluish-green emissive carbon dots. As shown in figure 7(b), the emission spectrum covered the whole visible range, and an excellent CRI of 96.2 was achieved. The CIE coordinate was located at (0.3700, 0.3970), with a CCT of 4411 K for warm white light at 50 mA. In addition, the white spectrum filled the range of 490–510 nm, where the human eye has the maximum sensitivity at night. Therefore, the fabricated white LED is expected to be efficient at nighttime illumination.

4. Conclusion

Fluorescent carbon dots with diameters of 3–5 nm were synthesized via the thermal carbonization of citric acid. The emission of these carbon dots strongly depended on the excitation wavelength, and the surface passivation played a crucial role in the luminescence properties. Because of the chemical similarity of the capped amine group, the optical properties of oil-soluble OAm- and HDA-capped carbon dots were nearly identical, while that of water-soluble MPA-capped carbon dots showed distinguishable features with a quantum yield loss. For practical application, a carbon dot-based color-conversion white LED was fabricated. When a 380nm UV LED was combined with the carbon dots and Zn-doped $AgInS_2$ NCs, an extremely high CRI greater than 95 with warm white light was achieved.

The results suggest that carbon dots could be applied to a white LED color converter, and offer great potential for further application in optoelectronic devices.

Acknowledgement

This research was supported by Basic Science Research Program through the National Research Foundation of Korea (NRF) funded by the Ministry of Education, Science and Technology (2012R1A1A2007908).

This work was supported by the Human Resources Development the Korea Institute of Energy Technology Evaluation and Planning (20114010203050) grant funded by the Korean government Ministry of Knowledge Economy.

References

[1] L. Li, A. Pandey, D. J. Werder, B. P. Khanal, J. M. Pietryga, and V. I. Klimov, *J. Am. Chem. Soc*. **133**, 1176–1179 (2011).

[2] W. Song and H. Yang, *Appl. Phys. Lett.* **100**, 1831041–1831044 (2012).

[3] J. Park and S.-W. Kim, *J. Mater. Chem.* **21**, 3745–3750 (2011).

[4] L. Li, T. J. Daou, I. Texier, T. Thi, K. Chi, N. Q. Liem, and P. Reiss, *Chem. Mater.* **21**, 2422–2429 (2009).

[5] L. Tian, H. Elim, W. Ji, and J. Vittal, *Chem. Commun*., 4276–4278 (2006).

[6] T. Torimoto, T. Adachi, K. Okazaki, M. Sakuraoka, T. Shibayama, B. Ohtani, A. Kudo, and S. Kuwabata, *J. Am. Chem. Soc.* **129**, 12388–12389 (2007).

[7] B. Mao, C. Chuang, J. Wang, and C. Burda, *J. Phys. Chem. C* **115**, 8945–8954 (2011).

[8] X. Tang, K. Yu, Q. Xu, E. Shi, G. Choo, G. Goh, and J. Xue, *J. Mater. Chem*. **21**, 11239–11243 (2011).

[9] X. Tang, W. Ho, and J. Xue, *J. Phys. Chem. C* **116**, 9769−9773 (2012).

[10] B. Mao, C. Chuang, F. Lu, L. Sang, J. Zhu, and C. Burda, *J. Phys. Chem. C* **117**, 648−656 (2013).

[11] X. Yang, Y. Tang, S. Tan, M. Bosman, Z. Dong, K. Leck, Y. Ji, H. Demir, and X. Sun, *Small* **9**, 2689–2695 (2013).

[12] Y. Sun, B. Zhou, Y. Lin, W. Wang, K. Fernando, P. Pathak, M. Meziani, B. Harruff, X. Wang, H. Wang, P. Luo, H. Yang, M. Kose, B. Chen, L. Veca, and S. Xie, *J. Am. Chem. Soc*. **128**, 7756–7757 (2006).

[13] H. Li, X. He, Z. Kang, H. Huang, Y. Liu, J. Liu, S. Lian, C. Tsang, X. Yang, and S. Lee *Angew. Chem. Int. Ed.* **49**, 4430–4434 (2010).

[14] H. Li, Z. Kang, Y. Liu, and S. Lee, *J. Mater. Chem.* **22**, 24230–24253 (2012).

[15] S. Qu, X. Wang, Q. Lu, X. Liu, and L. Wang, *Angew. Chem. Int. Ed.* **51**, 12215–12218 (2012).

[16] Y. Liu, C. Liu, and Z. Zhang, *J. Mater. Chem. C* **1**, 4902–4907 (2013).

[17] P. Luo, S. Sahu, S. Yang, S. Sonkar, J. Wang, H. Wang, G. LeCroy, L. Cao, and Y. Sun, *J. Mater.*

Chem. B **1,** 2116–2127 (2013).

[18] X. Xu, R. Ray, Y. Gu, H. Ploehn, L. Gearheart, K. Raker, and W. Scrivens, *J. Am. Chem. Soc.* **126**, 12736–12737 (2004).

[19] X. Y. Li, H. Q. Wang, Y. Shimizu, A. Pyatenko, K. Kawaguchi, and N. Koshizaki, *Chem. Commun.* **47**, 932–934 (2011).

[20] S. L. Hu, K. Y. Niu, J. Sun, J. Yang, N. Q. Zhao, and X. W. Du, *J. Mater. Chem.* **19**, 484–488 (2009).

[21] F. Wang, S. Pang, L. Wang, Q. Li, M. Kreiter, and C. Liu, *Chem. Mater*. **22**, 4528–4530 (2010).

[22] F. Wang, Y. Chen, C. Liu, and D. Ma, *Chem. Commun*. **47**, 3502–3504 (2011).

[23] H. Q. Tao, K. Yang, Z. Ma, J. M. Wan, Y. J. Zhang, Z. H. Kang, and Z. Liu, *Small* **8**, 281–290 (2012).

[24] J. Zong, Y. H. Zhu, X. L. Yang, J. H. Shen, and C. Z. Li, *Chem. Commun.* **47**, 764 (2011).

[25] X. Zhang, Y. Zhang, Y. Wang, S. Kalytchuk, S. Kershaw, Y. Wang, P. Wang, T. Zhang, Y. Zhao, H. Zhang, T. Cui, Y. Wang, J. Zhao, W. Yu, and A. Rogach, *ACS Nano* **12**, 11234-11241 (2013).

[26] X. Guo, C. Wang, Z. Yu, L. Chen, and S. Chen, *Chem. Commun*. **48**, 2692–2694 (2012).

[27] W. Kwon, S. Do, J. Lee, S. Hwang, J. Kim, and S. Rhee, *Chem. Mater*. **25**, 1893−1899 (2013).

[28] Y. Jun, S. Lee, N. Kang, and J. Cheon, *J. Am. Chem. Soc*. **123**, 5150–5151 (2001).

[29] K. Leschkies, R. Divakar, J. Basu, E. Enache-Pommer, J. Boercker, C. Carter, U. Kortshagen, D. Norris, and E. Aydil, *Nano Lett*. **7**, 1793–1798 (2007).

Figure 1. HR-TEM images of (a) HDA-capped carbon dots and (c) OAm-capped carbon dots prepared at 300°C.

Figure 2. ATR FT-IR spectra of (a) MPA- (b) HDA-, and (c) OAm-capped carbon dots.

Figure 3. Absorption and emission spectra of (a) HDA- (b) OAm-, and (c) MPA-capped carbon dots with different excitation wavelengths.

Figure 4. Maximum emission peaks with different pyrolysis temperatures of 200, 250, and 300°C, and corresponding HR-TEM images of obtained carbon dots.

Figure 5. Emission spectra of (a) $AgInS_2$ NCs with increasing temperature and (b) Zn-doped $AgInS_2$ NCs with different Zn:Ag ratios.

Figure 6. (a) Powder XRD patterns of pure $AgInS_2$ NCs and Zn-doped $AgInS_2$ NCs (Zn/Ag = 4). HR-TEM image of (b) $AgInS_2$ and (c) Zn doped $AgInS_2$ NCs (Zn/Ag = 4).

Figure 7. Emissions of white LED fabricated by combining (a) 430nm LED with carbon dots and (b) 380nm UV LED with carbon dots and Zn-doped $AgInS_2$ NCs.

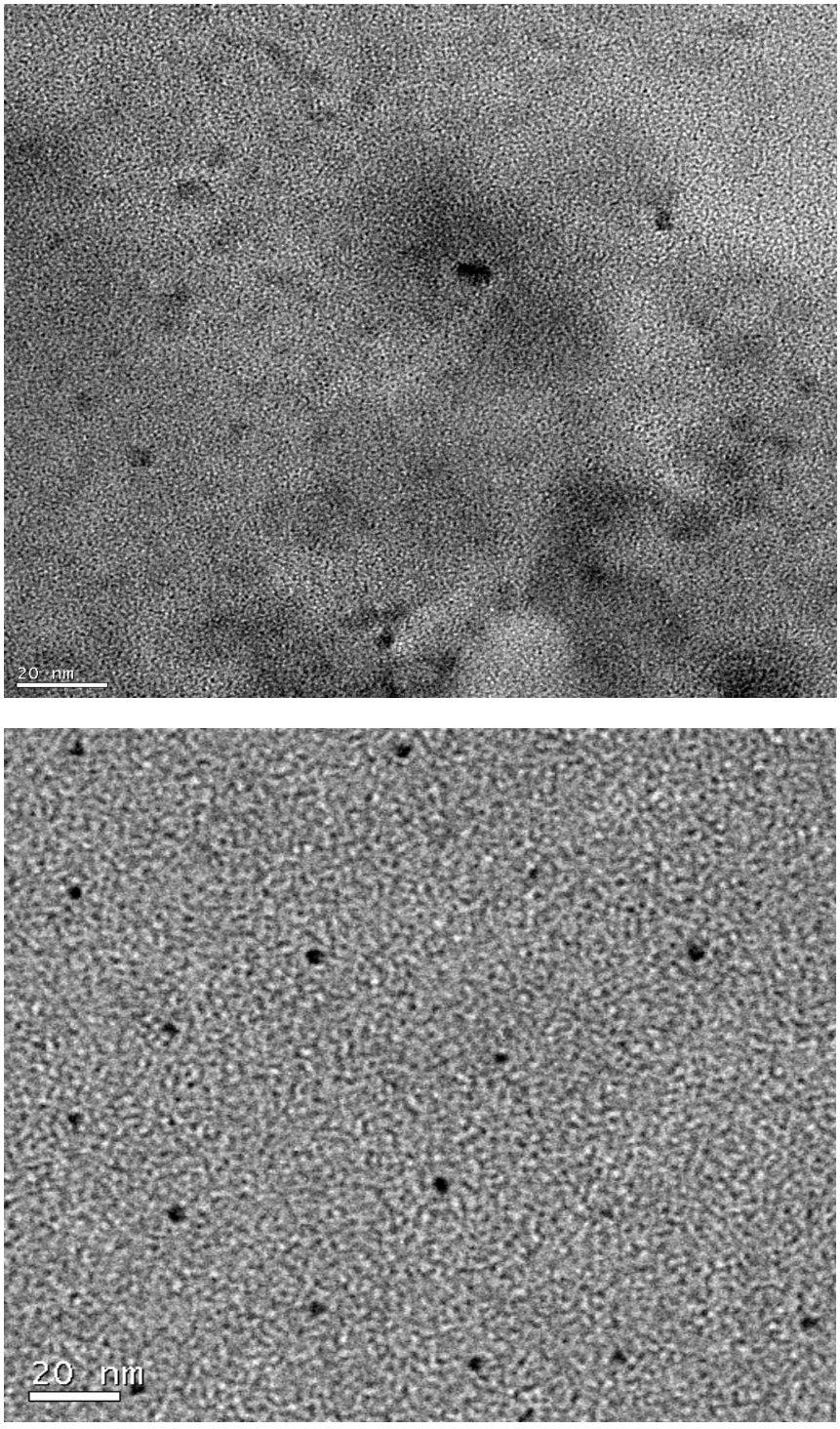

Figure 1. HR-TEM images of (a) HDA-capped carbon dots and (c) OAm-capped carbon dots prepared at 300°C.

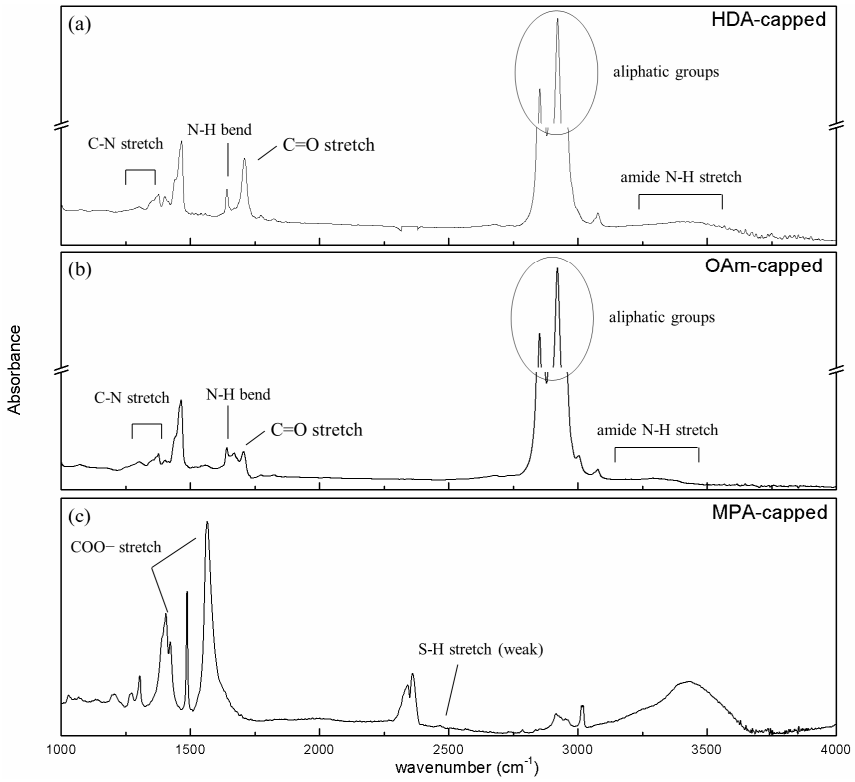

Figure 2. ATR FT-IR spectra of (a) MPA- (b) HDA-, and (c) OAm-capped carbon dots.

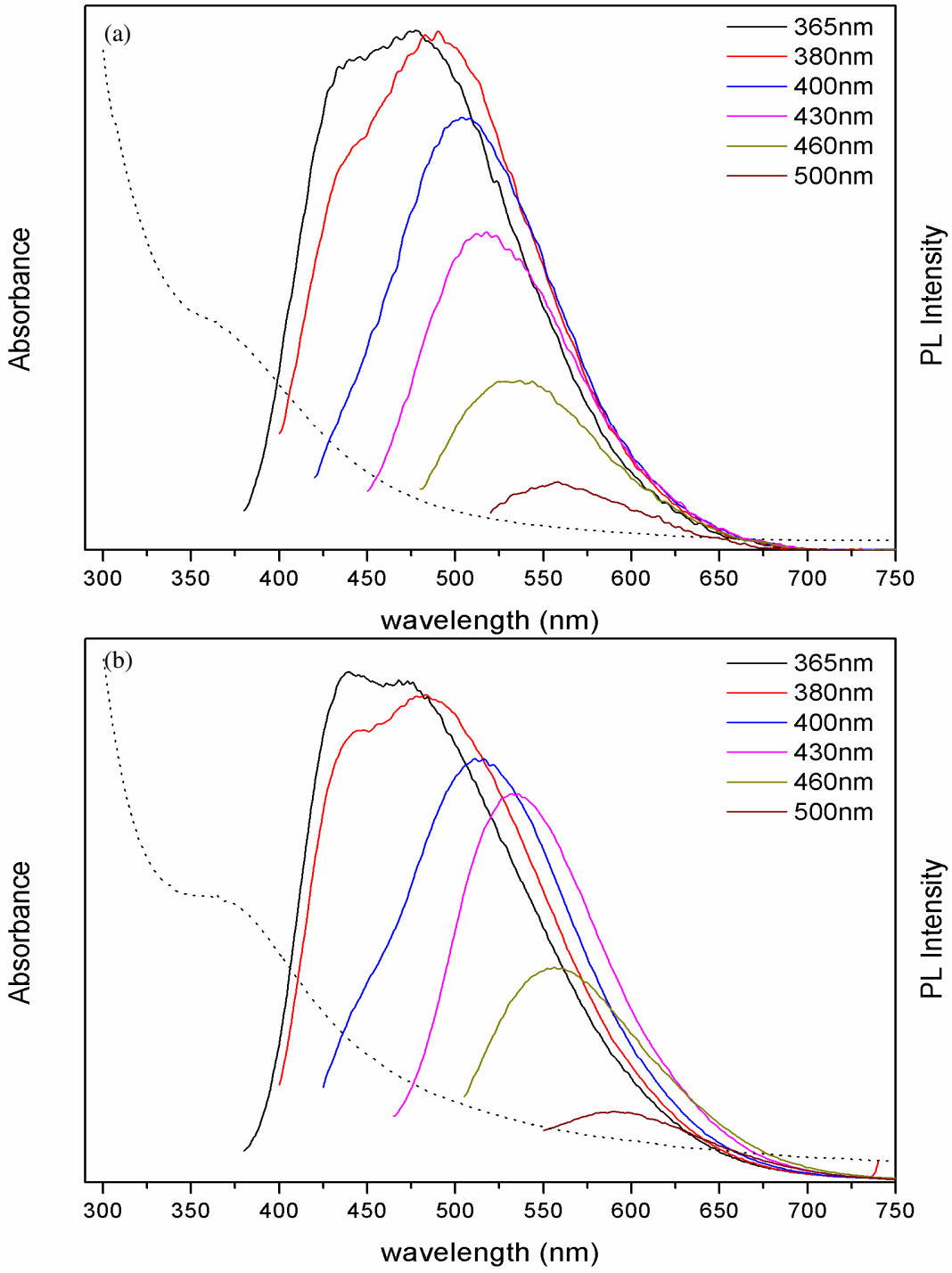

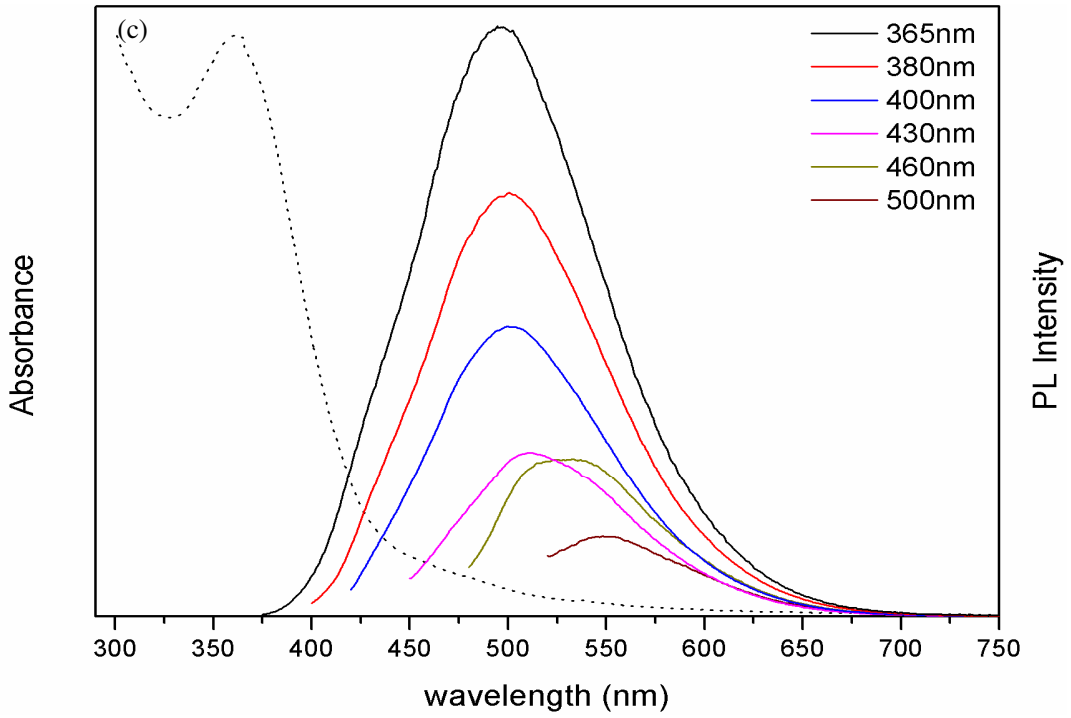

Figure 3. Absorption and emission spectra of (a) HDA- (b) OAm-, and (c) MPA-capped carbon dots with different excitation wavelengths.

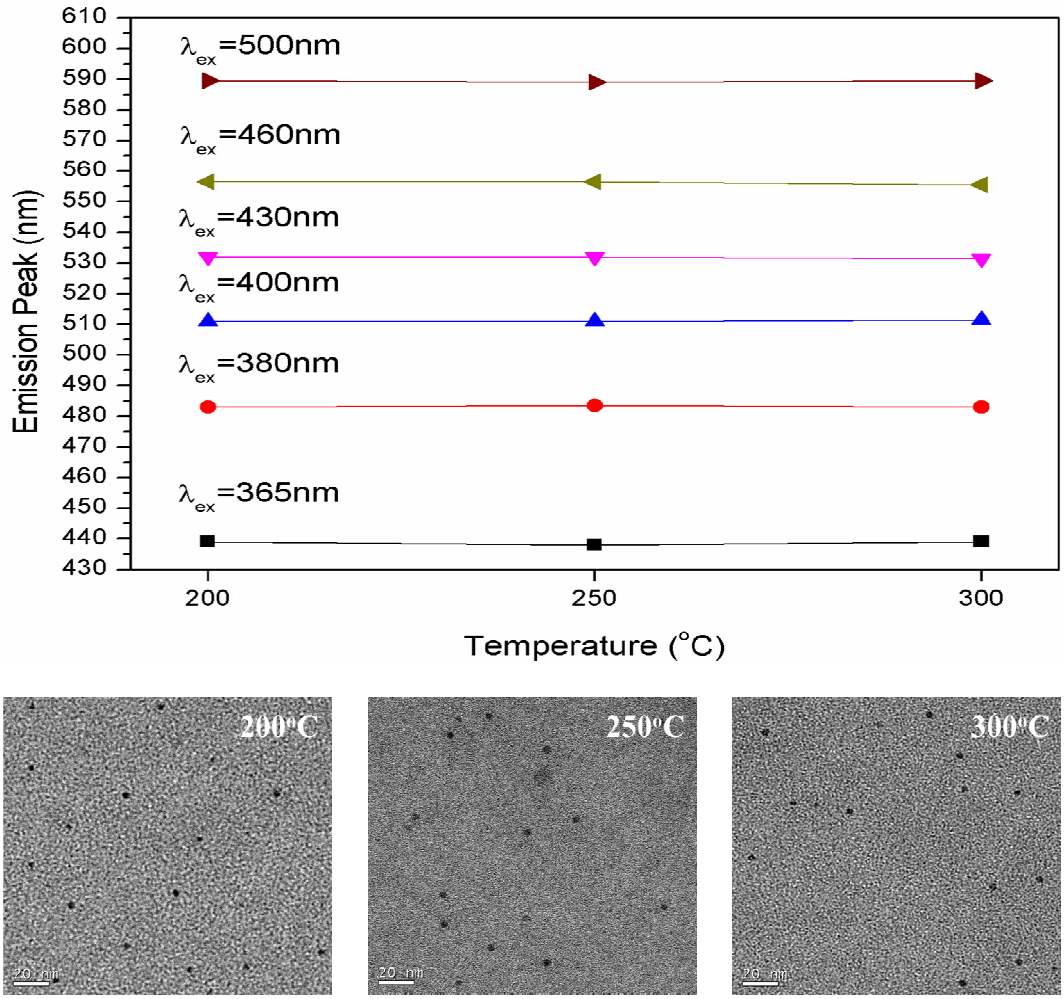

Figure 4. Maximum emission peaks with different pyrolysis temperatures of 200, 250, and 300°C, and corresponding HR-TEM images of obtained carbon dots.

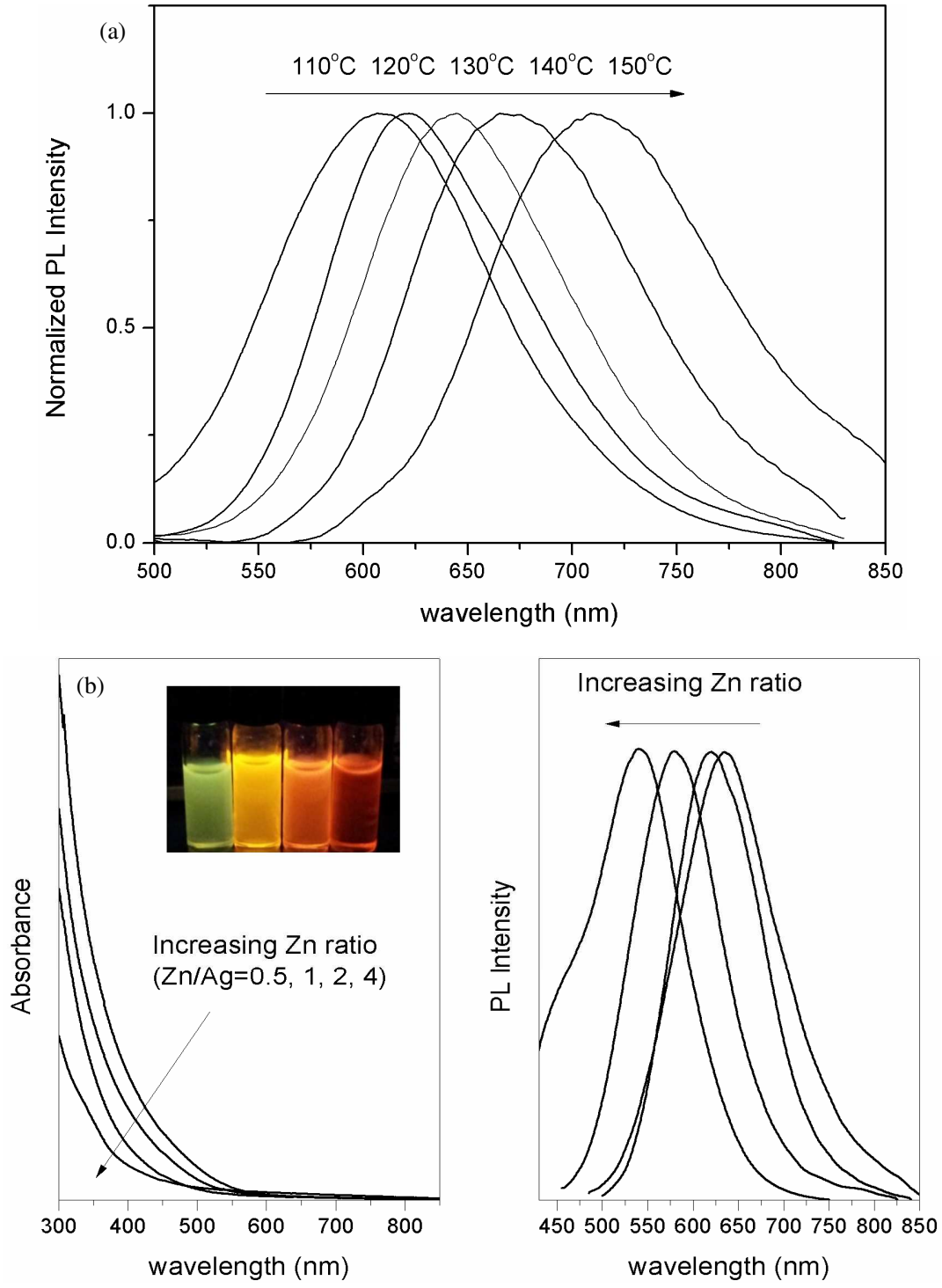

Figure 5. (a) Emission spectra of $AgInS_2$ NCs with increasing temperature and (b) absorption and emission of Zn-doped $AgInS_2$ NCs with different Zn:Ag ratios.

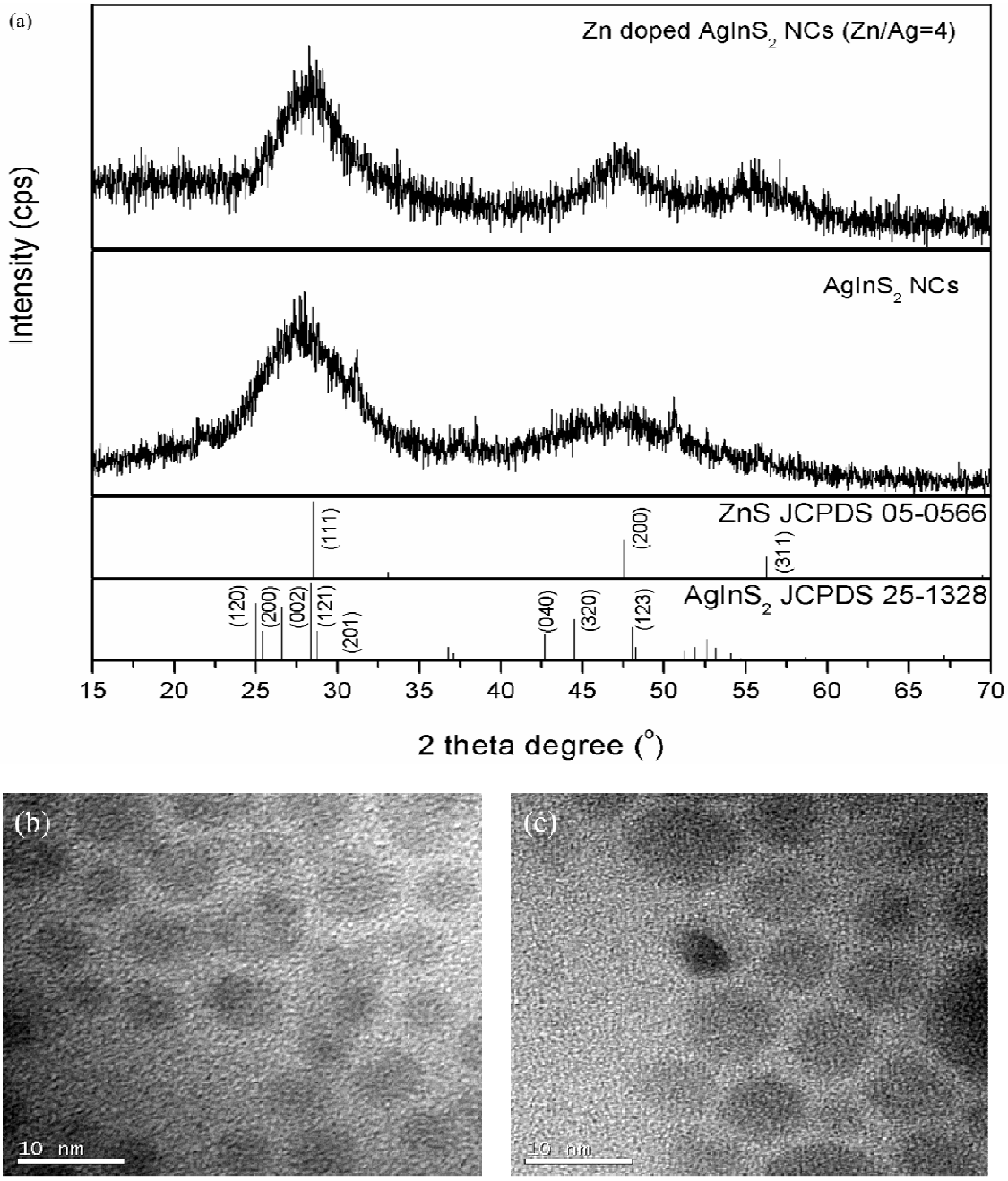

Figure 6. (a) Powder XRD patterns of pure $AgInS_2$ NCs and Zn-doped $AgInS_2$ NCs (Zn/Ag = 4).

HR-TEM image of (b) $AgInS_2$ and (c) Zn doped $AgInS_2$ NCs (Zn/Ag = 4).

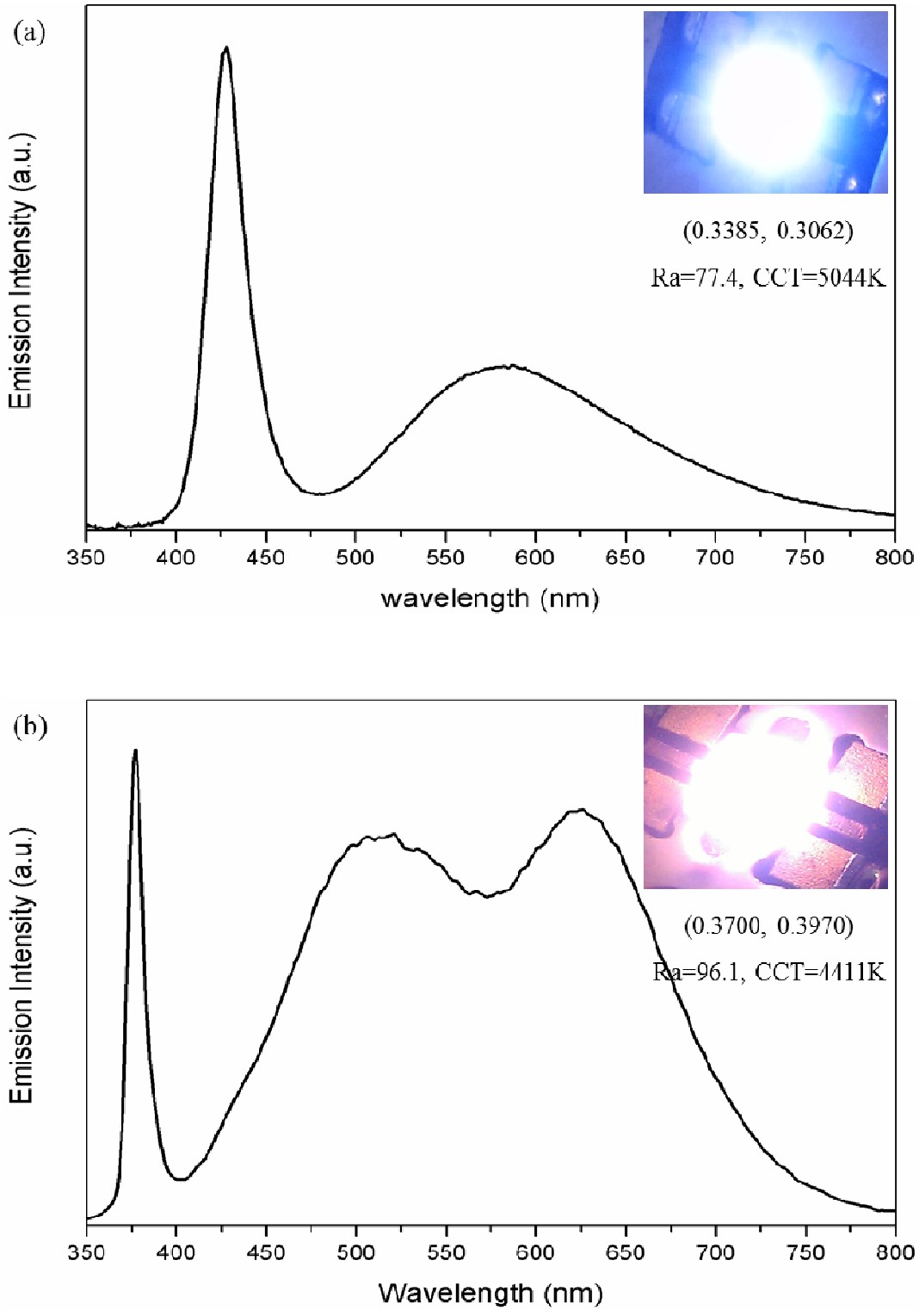

Figure 7. Emissions of white LED fabricated by combining (a) 430nm LED with carbon dots and (b) 380nm UV LED with carbon dots and Zn doped $AgInS_2$ NCs.